# Revisiting Albarracín Rock Art Through Multivariate pXRF Analysis of White, Black, and Red Pigments

Pablo Martín-Ramos, José Antonio Cuchí-Oterino, and Manuel Bea-Martínez

SUPPORTING INFORMATION

## GUIDE TO SUPPORTING INFORMATION ORGANIZATION

This Supporting Information document provides comprehensive details for the multivariate and univariate statistical analyses presented in the main manuscript.

**Document structure:**

### *Section S1: Shelter descriptions and archaeological context*

Detailed descriptions of each of the 12 rock art shelters, including archaeological context, preserved motifs, conservation state, and tracings showing sampling point locations (Figures S1-S12).

### *Section S2: Raw and transformed data*

- Table S1: Raw elemental composition data for all pigment samples.
- Table S2: Elemental composition of unpainted rock substrates by shelter.
- Table S3: Z-scores of CLR-transformed data for 15 compositional variables.

### *Section S3: Statistical results by pigment type*

- White pigments: Tables S4-S11.
- Black/layered pigments: Tables S12-S19.
- Red pigments: Tables S20-S27.

## S1. DETAILED DESCRIPTION OF STUDIED ROCK ART SHELTERS

### *S1.1. Cabras Blancas*

It is located near the Tormón meadow, within the same sandstone massif that contains the shelters of Cerrada del Tío Jorge and Ceja de Piezarrodilla. However, its position on the opposite slope to these sites confines the immediate context of the shelter to a gentle hillside populated with tall pine trees. Nevertheless, just 10 meters to the east of the shelter offers one of the most beautiful views over the Tormón meadow. On the main panel, a total of 14 figures are visible: nine goats (both males and females) and five anthropomorphic representations. The white color of the representations contrasts with the black background of the ceiling on which they were created. Within a rather small area, less than one square meter, a dynamic scene unfolds in which it is possible to observe the distinct graphic treatment applied to animals and humans. A herd of nine goats is depicted with a marked naturalistic style. The ears, hooves, antlers (in a semi-twisted perspective), hocks, and well-proportioned bodies are clearly defined, though the artist seems to have allowed for certain stylistic liberties, such as an exaggerated neck and slightly smaller head in some of the figures. The various postures of the animals capture the dynamic force of the scene. While some appear to wait for events to unfold, others are seen running, or shown with their legs folded, wounded or dead, as evidenced by the arrows embedded in their bodies.

The action is complemented by human figures. Up to five anthropomorphic representations are included in the scene, sharing the same dynamic energy as the animals, running after them and, in some cases, armed with bows. The hunting theme of the ensemble is clear, though what stands out is the distinct stylistic treatment of the human figures, a characteristic common to prehistoric rock art. The anthropomorphs are depicted in highly stylized forms, with linear bodies slightly widened at the top to represent the shoulders, small, elongated globular heads, and limbs reduced to mere strokes with no anatomical treatment, except for a short line representing the foot. However, despite this formal simplicity, the limbs and bodies of the anthropomorphs possess great dynamic strength due to the curvature of their lines, giving the impression that they are floating.

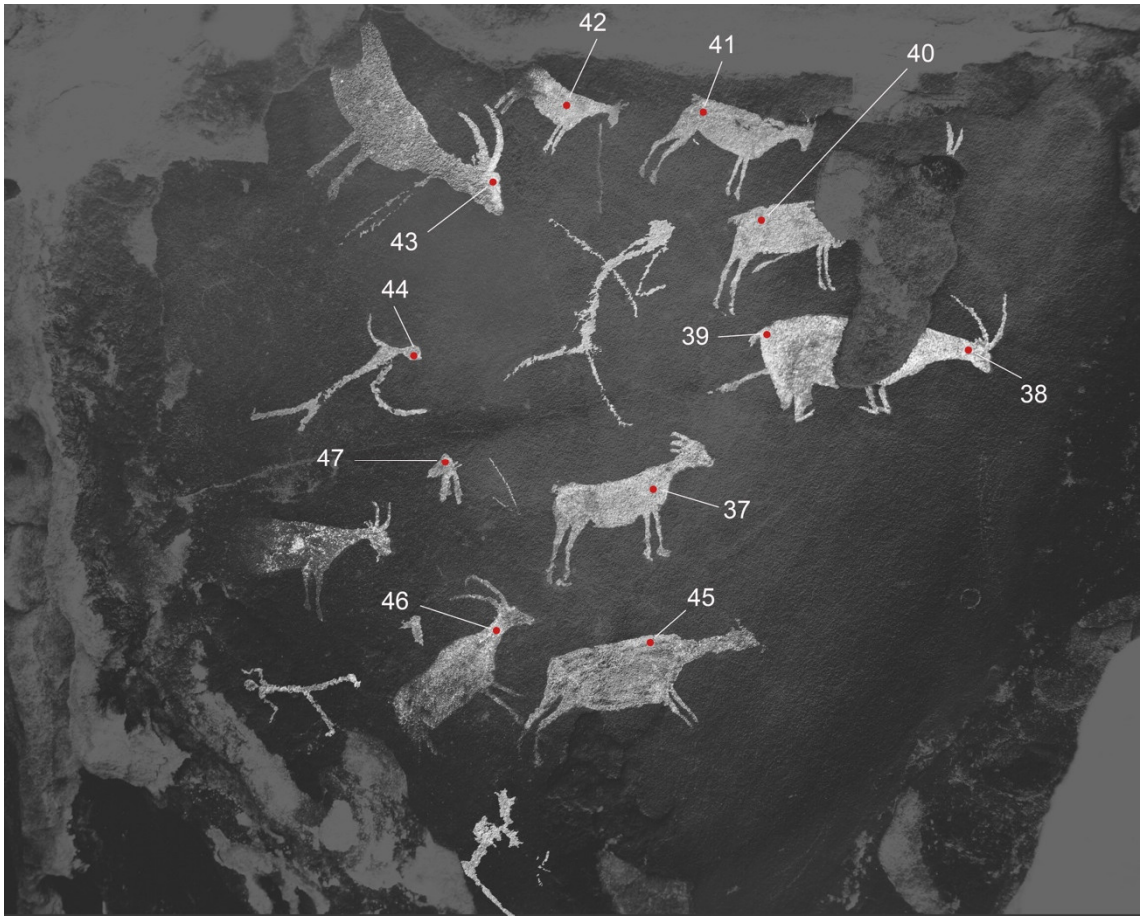



**Figure S1**. Digital tracings of analyzed paintings from the Cabras Blancas shelter showing sampling points.

### *S1.2. Casa Forestal I*

The decorated panel is located at the base of the upper section of a large rock formation, oriented W/SW, with excellent visibility from the valley floor. It is also protected by a substantial visor. The panel measures 128 cm in length and 90 cm in height, with the representations situated 60 cm above the present ground level.

A total of seven whitish-toned figures were executed. Overall, the zoomorphic figures dominate the thematic content of the panel, including an indeterminate quadruped, as well as a goat and a deer oriented to the right, both slender in form. Particularly noteworthy is the finely rendered head and neck of a small hind, executed with great attention to detail: two upright ears, a naturalistic tendency, and a long, slender snout.

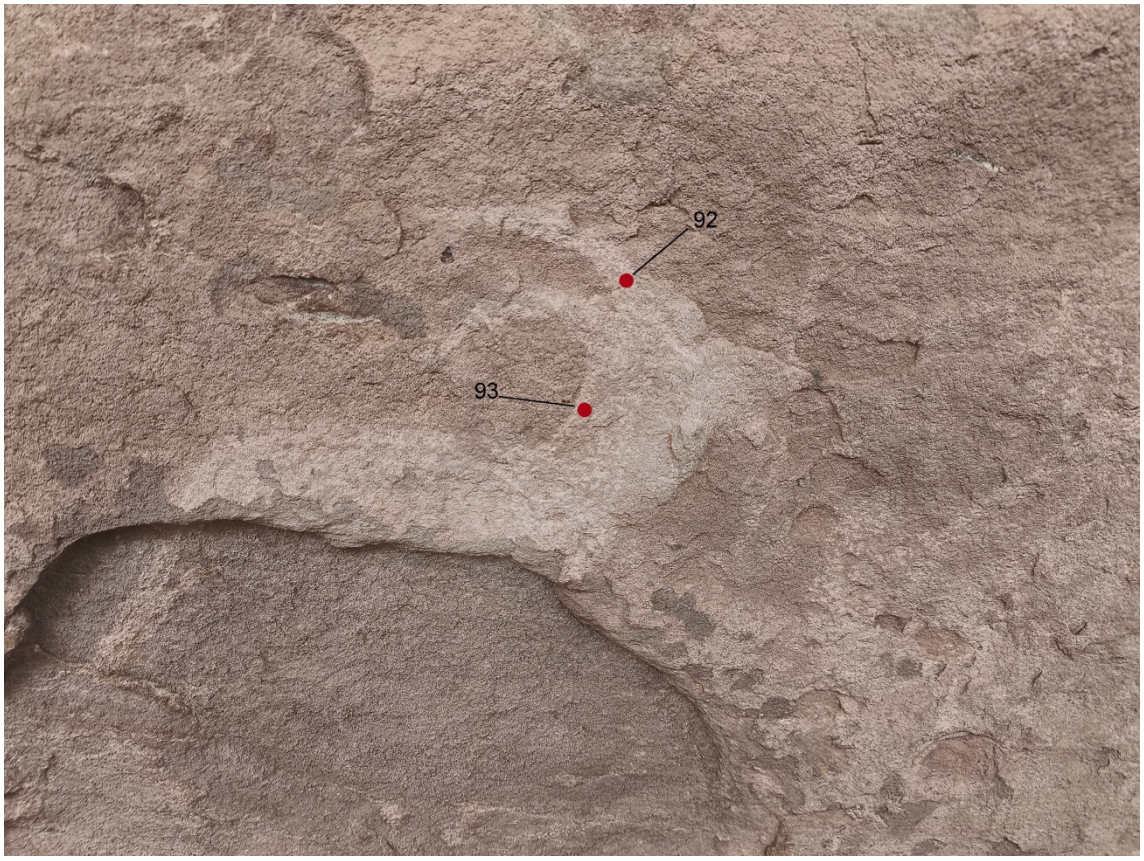



**Figure S2**. Original picture of analyzed paintings from Casa Forestal I shelter showing sampling points.

### *S1.3. Casa Forestal II*

This shelter, oriented to the NE, is relatively complex, owing to the abundance of motifs and the observed stylistic and chromatic variety. Thus, we find indeterminate motifs in whitish and red tones, along with others identifiable as signs, featuring a linear morphology with a diagonal trajectory ascending toward the right, terminating in rounded lobes at each end.

Another motif is a closed, rectangular-shaped sign, inside of which—particularly on the right side—a series of vertical parallel strokes can be discerned. Some of these extend beyond the rectangular frame, continuing downward.

Among the figurative motifs, there is a massive-bodied quadruped lacking detailed anatomy and without its head represented. Of particular interest is the depiction of a goat's head, located beneath some red strokes that may be associated with another possible goat's head facing left. In this same area, additional red traces may represent poorly preserved remains of an animal's body, in direct association with the goat heads. This combination results in a very interesting interplay of chromatic and stylistic elements, ultimately forming a single representation.

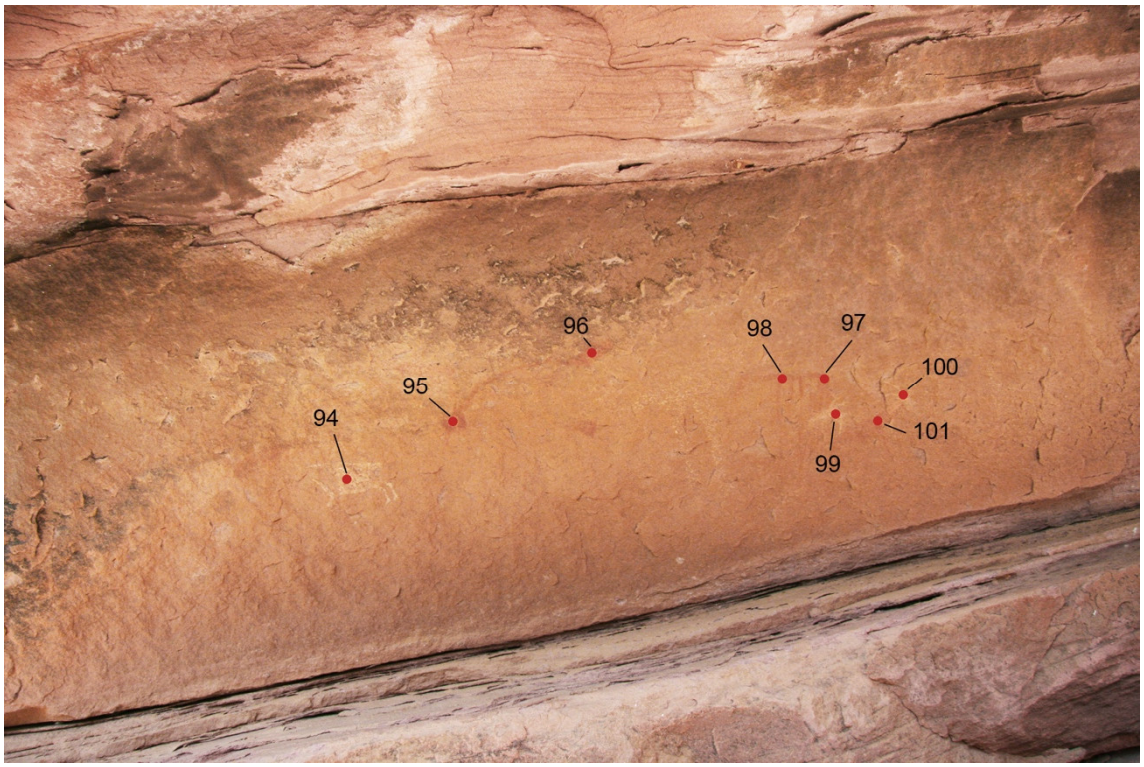



**Figure S3**. Original picture of analyzed paintings from Casa Forestal II shelter showing sampling points.

### *S1.4. Casa Forestal V*

The shelter of Casa Forestal V is situated in an unusual formation, almost resembling a sort of "monolith", near the shelter of Casa Forestal I. On the panel, only a very faded representation of a quadruped (possibly a cervid) with a naturalistic tendency has been preserved.

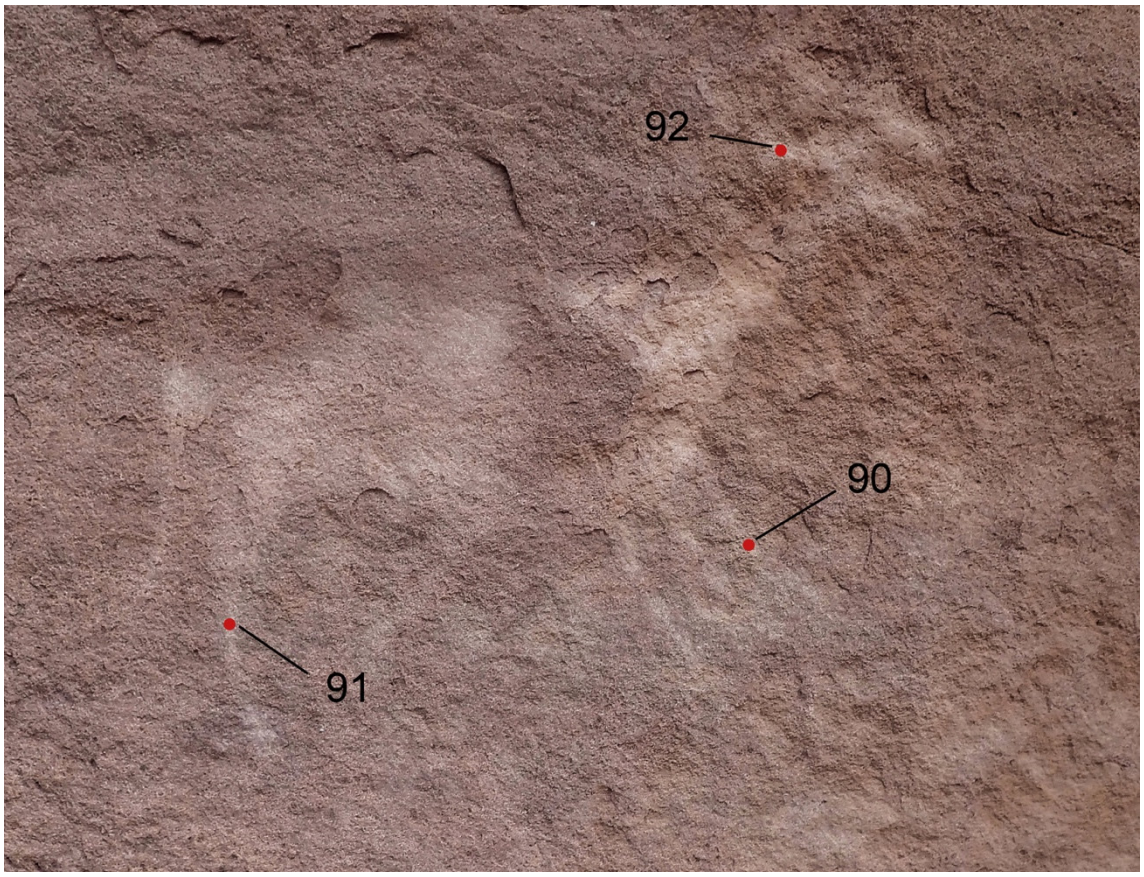



**Figure S4**. Digital tracings of analyzed paintings from Casa Forestal V shelter showing sampling points.

### *S1.5. Ceja de Piezarrodilla*

This shelter presents one of the most complex and intriguing rock art assemblages in the Sierra de Albarracín, characterized by multiple painting episodes and diverse chromatic treatments. The site has been the subject of considerable scholarly attention due to the exceptional quality and complexity of its representations. The site was discovered by Breuil in 1926, with preliminary notice given in a brief article published by Obermaier [1] and subsequently published by both researchers [2]. It would later be mentioned again in the works of Beltrán [3,4], although without in-depth analysis or new tracings, analytical work that was carried out in studies developed by Piñón [5,6]. In recent years, it has been the subject of new documentation and study [7] with a novel interpretative proposal.

Two different panels are located in the shelter. The first contains the representation of a large bull that follows a proportional pattern removed from the purest realism of representations in other Levantine assemblages, displaying an excessively elongated body relative to the legs. However, it presents a series of naturalistic features such as the detail of the ear, hump, or tail, which is long and plumed. It is worth highlighting the observed difference between the two pairs of preserved horns, through which it is possible to argue for the existence of a global repainting of the motif. Thus, two horns in twisted perspective of white color are visible in the center of the animal's head. These would constitute, along with barely perceptible remains in different areas of the animal's front half, the only preserved elements of the original motif. Over this figure, a repainting in black

color was executed that, in essence, would retrace the form of the previous zoomorph except for the horns, for which a new arrangement and perspective were employed. In this second phase, much finer and more realistic antlers were created, lyre-shaped, although still in frontal perspective.

In Panel 2, a second zoomorphic representation is located, partially preserved, of whitish tonality.

Perhaps the most noteworthy aspect could be the revised reading of the bovid in Panel 1. Thus, the possibility is suggested that the orange remains alluded to in previous studies were, in reality, the visual component of a progressive degradation process motivated, perhaps, by the growth of lichens or cyanobacteria, whose initial growth processes would correspond to the description made by Piñón and which, over time, would have become generalized throughout the entire figure. This would not constitute, therefore, a differentiated decorative phase but rather a degenerative process of the paint due to the emergence of lichens or cyanobacteria.

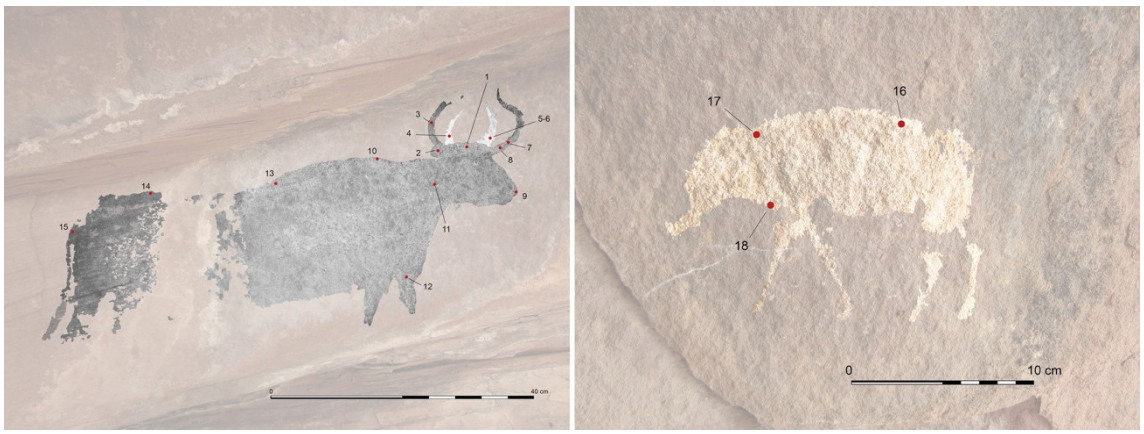



**Figure S5**. Digital tracings of analyzed paintings from the Ceja de Piezarrodilla shelter showing sampling points.

### *S1.6. Hoya de Navarejos II*

In this group, only a single whitish-toned representation has been documented, identified as a human figure. It is a stylized anthropomorphic figure, standing upright, with a globular-shaped head from which two small, vertical, parallel lines protrude from the top, resembling ornamental elements (possibly antennae or feathers). The body is linear, although a broadening is noticeable at the top, corresponding to the shoulders. The right arm is bent and holds a pair of curved elements grasped at their vertices (in the central area), with the ends pointing outward. The left arm is also bent, positioned slightly upward in relation to a long, thin diagonal line that could be interpreted as a staff or possibly a spear.




**Figure S6**. Original picture of analyzed paintings from Hoya de Navarejos II shelter showing sampling points.

### *S1.7. Hoya de Navarejos III*

The Hoya de Navarejos III site is one of the most outstanding rock art ensembles discovered in recent years [8]. The rock art ensemble is located in a sandstone formation whose compositional characteristics determine great vulnerability to erosive processes. The shelter opens at the top of a sandstone formation with gentle morphology, in which natural alteration processes determined the enlargement of fractures in the support that would culminate in the individualization of blocks. One of these blocks moved from the basal zone of the rock formation along a fracture line, adopting a transverse disposition at the very foot of the base rock. The lateral collapse and slight subsequent displacement of the block formed an interior space of reduced dimensions (273 cm in length, 79 cm in width, and 141 cm maximum height) with development parallel to the base rock. Inside this space, two decorated panels were created.

The first of these presents the representation of three large bovids in white color, which display stylistic characteristics typical of the area. At the final part of the gallery, the second decorated panel is located, with a greater number of figurations of smaller dimensions as well as different stylistic criteria and chromatism. The symbolic component of this panel is evident, documenting the head of a bull separated from the body, an indeterminate quadruped (perhaps a canid), part of a bovid body with representation of the ribs, and two highly stylized anthropomorphs, all executed in tonalities ranging from dark gray to black.

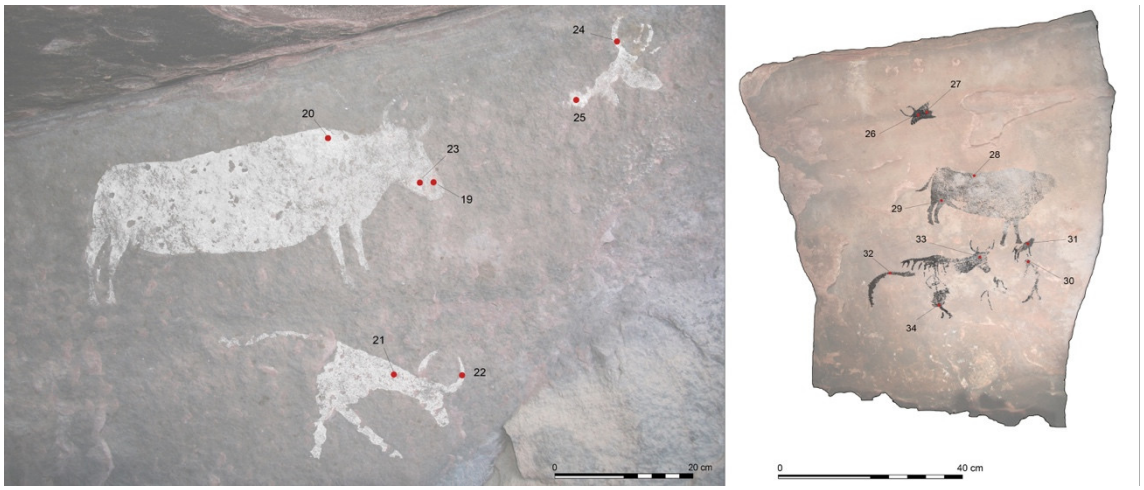



**Figure S7**. Digital tracings of analyzed paintings from Hoya de Navarejos III shelter showing sampling points.

### *S1.8. Hoya de Navarejos IV*

It is a set of very small dimensions. The panel measures 36 cm in width by 23 cm in height, and is protected only by a small visor 15 cm deep. The paintings are located 66 cm above the ground and are described as follows: a black cruciform and a black symbol composed of a vertical stroke with a thickening at its upper end, from which a small horizontal line extends to the left.




**Figure S8**. Digital tracing of analyzed paintings from Hoya de Navarejos IV shelter showing sampling points.

### *S1.9. Hoya de Navarejos V*

Alterations to the rock support have caused the practical disappearance of the totality of the representations, especially in the lower left area of the decorated panel. The erosive processes appear to be very active and seriously threaten the conservation of the remaining vestiges.

As a whole, it is possible to observe up to nine pictorial elements, some defined as unidentifiable remains or mere linear traces of red color; and others that are figurative, among which stands out a bovid in red color of carelessly executed style and rough appearance, as well as the antlers of a red deer, practically disappeared, whose dimensions and naturalism would approximate them to the specimens from the nearby Prao Medias shelter.

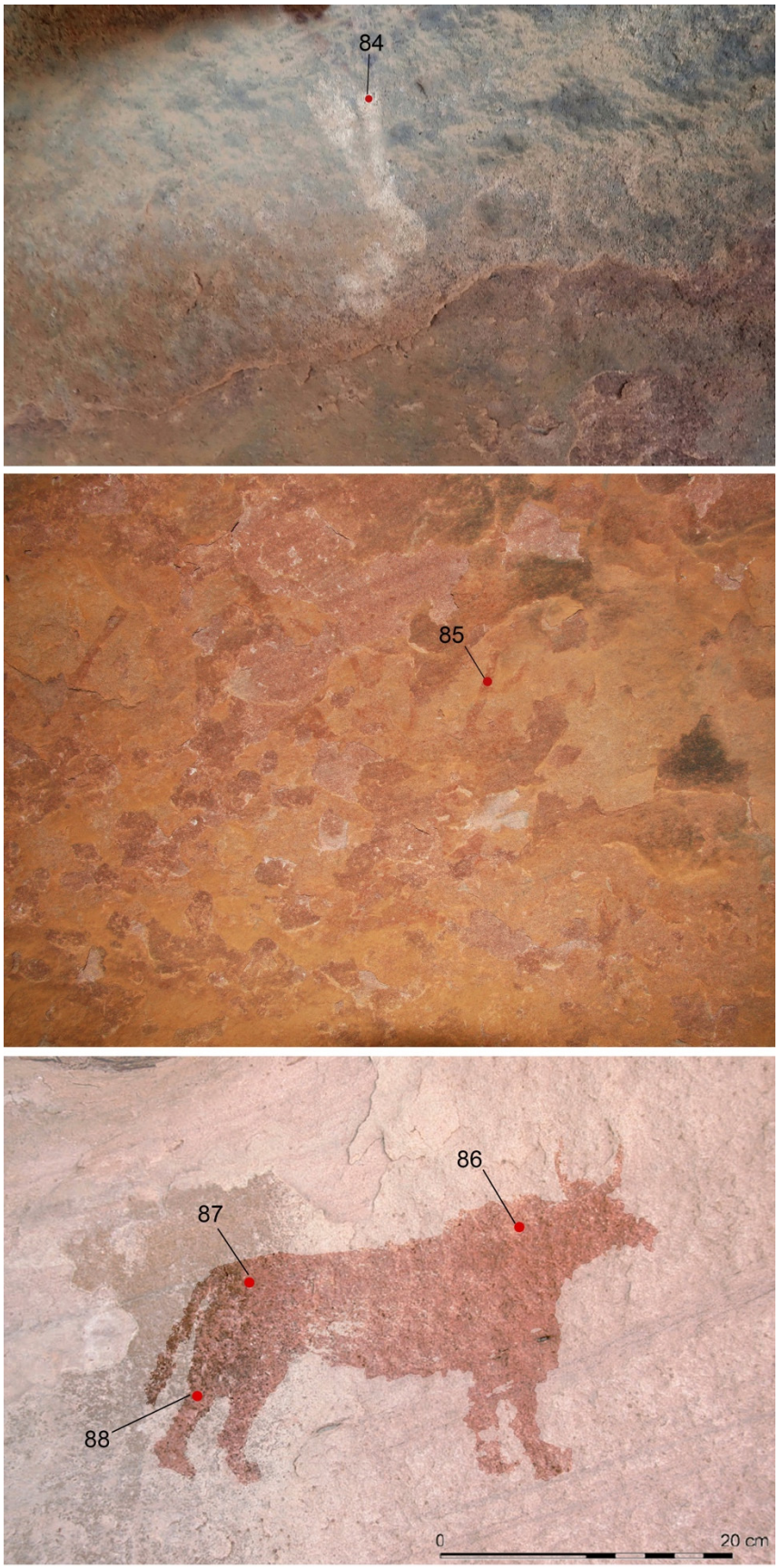



**Figure S9**. Digital tracing of analyzed paintings from Hoya de Navarejos V shelter showing sampling points.

### *S1.10. La Cocinilla del Obispo*

In classical studies, only six representations were identified, all of them bovids, a quantity and a theme that would be increased and diversified with Piñón's study [6]. In this work, ten representations are identified, of which eight correspond to bovid figures, one to an equid, and one compartmentalized rectangular sign of blackish tonality.

The representations are distributed across the frieze in three zones: on the left, the greatest number of animal figures are concentrated (five bulls and an equid), on the right, two bovids, and only one in the center. All the bull representations respond to similar stylistic approaches, although pigments of diverse tonalities were employed in their execution, ranging from whitish-yellow, through reddish and orange to black.

The preserved figure of the largest dimensions reaches 70 centimeters in length and is located at the left end of the frieze. The essentially naturalistic style of the figure reveals, however, some characteristics that distinguish it, appearing slightly disproportionate, with certain very marked anatomical details and a tendency toward figuration of the massive, robust, and elongated body. In all cases, the horns are semicircular (in frontal perspective), except for the figure occupying the center of the shelter, which presents lyre-shaped antlers.

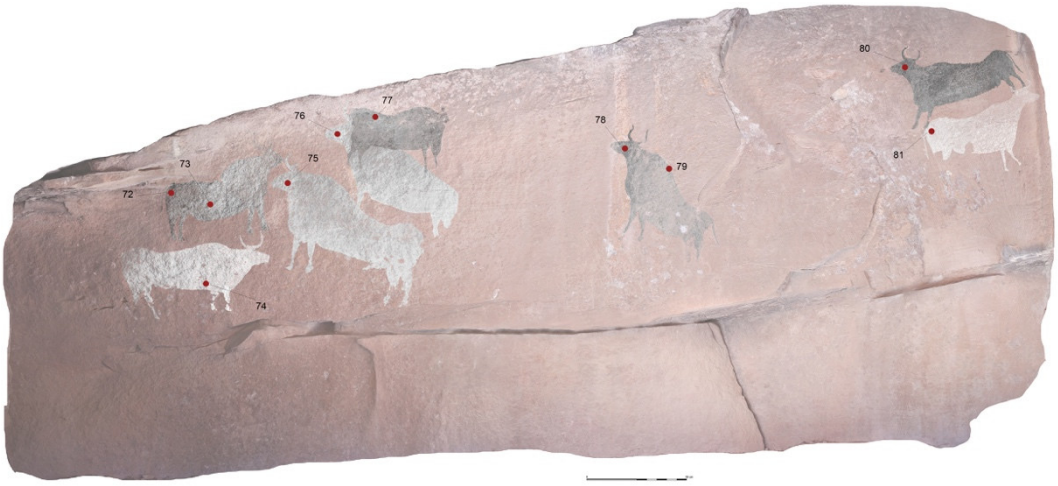



**Figure S10**. Digital tracings of analyzed paintings from La Cocinilla del Obispo shelter showing sampling points.

### *S1.11. Prado Navazo*

The Prado Navazo shelter represents one of the most significant concentrations of Levantine art representations in the Sierra de Albarracín. The site is characterized by an extensively decorated surface with multiple motifs executed primarily in white pigment, though other chromatic treatments are also present.

The shelter contains numerous representations of large-scale bovids, which constitute one of the most distinctive features of the Albarracín rock art tradition. These figures display the characteristic combination of naturalistic elements with stylistic conventions typical of Levantine art in this region. The paintings demonstrate varying degrees of preservation, with some motifs exceptionally well-preserved while others show evidence of natural deterioration processes affecting the rock substrate and pigment layers.

The analytical campaign documented a total of 18 white pigment samples, 3 black samples, making this shelter one of the most intensively sampled sites in the present study. This extensive sampling strategy was designed to capture the potential chemical variability within this large decorated ensemble and to investigate whether different painting episodes or material procurement strategies might be evident in the analytical data.

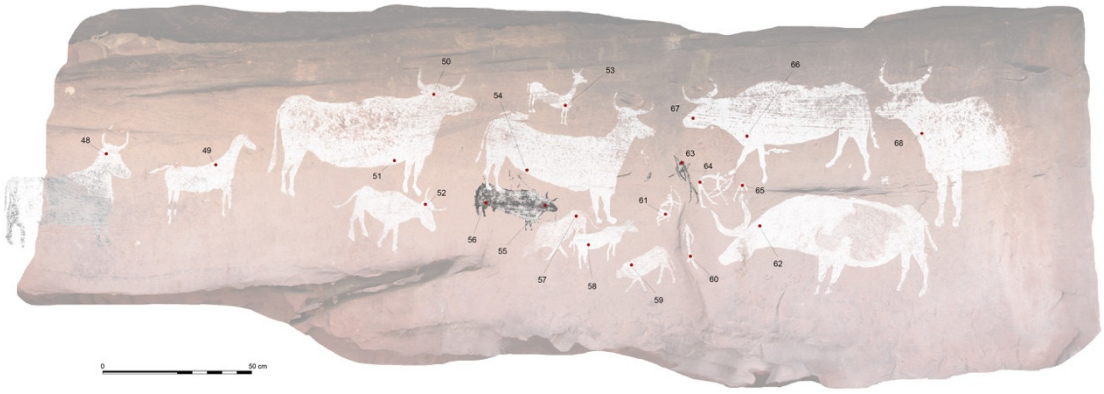



**Figure S11**. Digital tracings of analyzed paintings from the Prado Navazo shelter showing sampling points.

### *S1.12. Tío Campano*

The decorated shelter is located inside a cave complex that is easily accessible, without any obstacles or dangers, and provides good thermal insulation, making it habitable. The main panel, of relatively small dimensions, has a total length of 80 cm and a maximum height of 50 cm.

The poor state of conservation and the complexity of the superimposed representations have been notable obstacles to the proper definition of all the motifs in the ensemble, which has led to different and sometimes conflicting readings. Nevertheless, several figurations can be clearly identified, including a small equid (whose front legs are crossed and whose body is slightly inclined backward, giving the sensation of being in a rearing position) and a large anthropomorph represented schematically with rigid lines for the body, head, arms, and legs.

Apart from this figuration, there is another clearly identifiable as an equid of subnaturalistic style, without relevant anatomical details and with legs in oblique disposition. From the muzzle emerges a linear stroke in descending direction, which has led to discussion of a possible domestication scene. This stroke appears crossed by another in its lower third that develops obliquely in the direction of a cervid representation to end with a bifurcation into two short strokes.

The other two animal figures correspond to the image of two cervids that would participate in the same stylistic conventions. One of them preserves only part of the head and its characteristic antlers (with the typical schematic convention of two parallel vertical lines and short horizontal and parallel strokes to form the tines), while the other is presented practically complete, lacking only the front legs and muzzle.

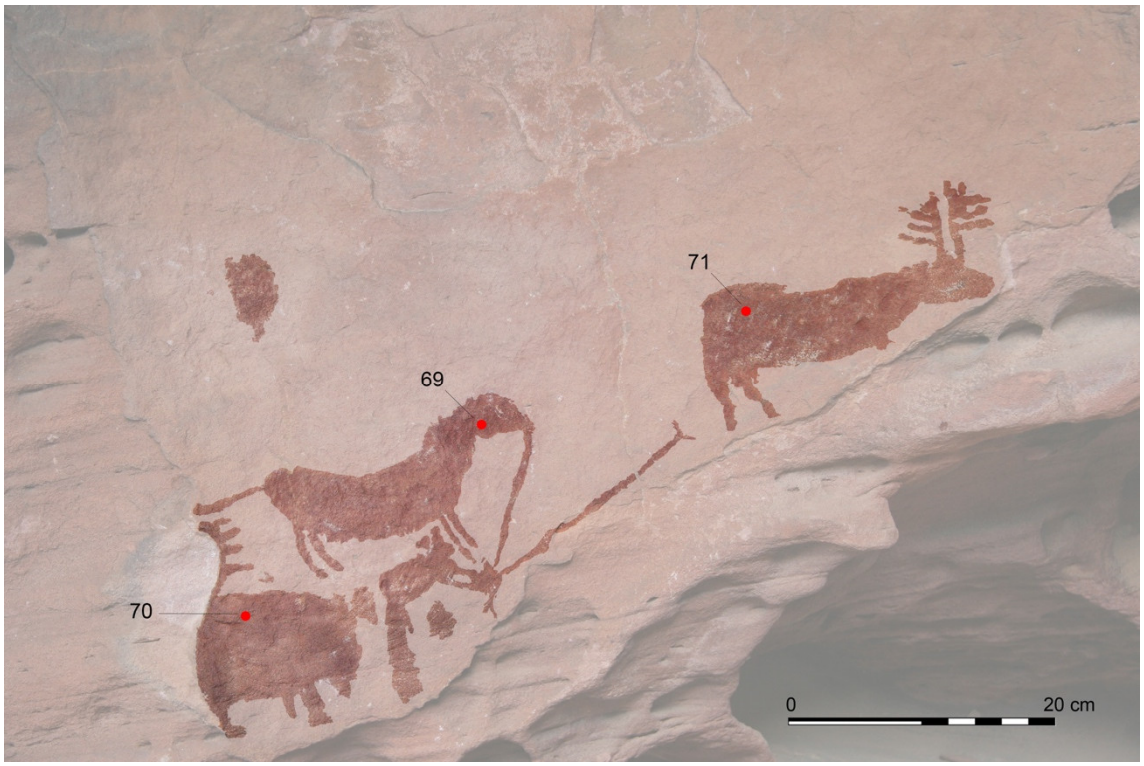



**Figure S12**. Digital tracing of analyzed paintings from the Tío Campano shelter showing sampling points.

## S2. RAW AND TRANSFORMED DATA

This section contains complete datasets and statistical outputs referenced throughout the main text, organized by pigment type (white, black/black-over-white/white-over-black, and red).

**Table S1.** Raw elemental composition data for all pigment samples (all elements detected). Values represent the mean of triplicate measurements. “Error” columns indicate the analytical uncertainty, i.e., the estimated ±2σ interval around the reported concentrations. 'Bal' denotes the balance fraction derived from undetected light elements (Z < Mg) required to sum the total composition to 100%.

[See separate Excel file]

**Table S2.** Elemental composition of unpainted rock substrates by shelter. Values represent the mean of triplicate measurements acquired on three representative unpainted areas at each shelter (n = 9 individual measurements per shelter). These substrate values serve as qualitative reference baselines for assessing pigment enrichment patterns rather than for mathematical background subtraction. Note: Representative rather than exhaustive characterization; substrate microheterogeneity is discussed in the main manuscript Section 4.5.

[See separate Excel file]

**Table S3.** Z-scores of CLR-transformed data for 15 compositional variables (all samples).

[See separate Excel file]

## S3. STATISTICAL RESULTS BY PIGMENT TYPE

### *White pigments*

**Table S4.** Principal component analysis results for white pigment samples (n = 54).

| Component | Eigenvalue | % Variance | Cumulative % |
|---|---|---|---|
| 1 | 5.864 | 39.092 | 39.092 |
| 2 | 5.073 | 33.819 | 72.911 |
| 3 | 2.026 | 13.508 | 86.419 |

**Table S5.** Factor loadings from the principal component analysis of white pigment samples.

| Element | Comp.1 | Comp.2 | Comp.3 |
|---|---|---|---|
| ZBa_CLR | −0.319 | −0.131 | −0.063 |
| ZBal_CLR | 0.233 | −0.352 | 0.054 |
| ZZr_CLR | 0.216 | 0.309 | −0.297 |
| ZSr_CLR | −0.329 | −0.153 | −0.333 |
| ZFe_CLR | 0.186 | −0.124 | −0.329 |
| ZMn_CLR | −0.217 | 0.163 | 0.510 |
| ZTi_CLR | 0.316 | 0.127 | 0.038 |
| ZCa_CLR | 0.19 | −0.355 | −0.016 |
| ZK_CLR | 0.229 | −0.265 | −0.141 |
| ZAl_CLR | 0.233 | −0.352 | 0.054 |
| ZP_CLR | 0.216 | 0.309 | −0.297 |
| ZSi_CLR | −0.329 | −0.153 | −0.333 |
| ZCl_CLR | 0.233 | −0.352 | 0.054 |
| ZS_CLR | 0.216 | 0.309 | −0.297 |
| ZMg_CLR | −0.329 | −0.153 | −0.333 |

**Table S6.** Sequential tests of discriminant functions for white pigment samples.

| Functions tested | Wilks' Λ | $\chi^2$ | df | p-value |
|---|---|---|---|---|
| 1 through 8 | 0.000 | 569.1 | 120 | < 0.001 |
| 2 through 8 | 0.000 | 414.14 | 98 | < 0.001 |
| 3 through 8 | 0.001 | 297.23 | 78 | < 0.001 |
| 4 through 8 | 0.007 | 201.98 | 60 | < 0.001 |

**Table S7.** Structure matrix - correlations between elements and discriminant functions for white pigment samples.

| Element | LD1 | LD2 | LD3 | LD4 | LD5 | LD6 | LD7 | LD8 | Highest function |
|---|---|---|---|---|---|---|---|---|---|
| ZBa_CLR | −0.852 | 0.237 | 0.310 | 0.148 | 0.186 | −0.048 | −0.246 | 0.048 | 1 |
| ZBal_CLR | 0.641 | 0.299 | 0.332 | −0.005 | 0.303 | −0.087 | −0.538 | −0.022 | 1 |
| ZZr_CLR | 0.274 | −0.092 | −0.583 | 0.094 | −0.290 | −0.340 | 0.246 | 0.554 | 3 |
| ZSr_CLR | −0.637 | −0.163 | 0.536 | −0.237 | 0.246 | 0.225 | −0.038 | 0.334 | 1 |
| ZFe_CLR | 0.381 | −0.302 | 0.162 | −0.686 | −0.046 | −0.476 | −0.195 | 0.006 | 4 |
| ZMn_CLR | −0.360 | 0.037 | −0.048 | 0.317 | 0.024 | 0.205 | 0.574 | −0.627 | 8 |
| ZTi_CLR | 0.618 | −0.332 | −0.495 | −0.046 | −0.408 | 0.068 | −0.290 | −0.075 | 1 |
| ZCa_CLR | 0.454 | 0.474 | 0.144 | −0.184 | 0.449 | −0.011 | −0.554 | 0.077 | 7 |
| ZK_CLR | 0.498 | 0.442 | 0.302 | −0.522 | −0.215 | −0.159 | −0.347 | 0.033 | 4 |
| ZAl_CLR | 0.641 | 0.299 | 0.332 | −0.005 | 0.303 | −0.087 | −0.538 | −0.022 | 1 |
| ZP_CLR | 0.274 | −0.092 | −0.583 | 0.094 | −0.290 | −0.340 | 0.246 | 0.554 | 3 |
| ZSi_CLR | −0.637 | −0.163 | 0.536 | −0.237 | 0.246 | 0.225 | −0.038 | 0.334 | 1 |
| ZCl_CLR | 0.641 | 0.299 | 0.332 | −0.005 | 0.303 | −0.087 | −0.538 | −0.022 | 1 |
| ZS_CLR | 0.274 | −0.092 | −0.583 | 0.094 | −0.290 | −0.340 | 0.246 | 0.554 | 3 |
| ZMg_CLR | −0.637 | −0.163 | 0.536 | −0.237 | 0.246 | 0.225 | −0.038 | 0.334 | 1 |

**Table S8.** Pairwise Euclidean distance matrix between white pigment sampling locations based on mean elemental compositions (n = 54 samples, 9 locations).

| | Casa Forestal I | Casa Forestal II | Casa Forestal V | Ceja de Piezarrodilla | Hoya de Navarejos II | Hoya de Navarejos III | Hoya de Navarejos V | La Cocinilla del Obispo | Prado Navazo |
|---|---|---|---|---|---|---|---|---|---|
| Casa Forestal I | 0.00 | 3.47 | 2.36 | 6.19 | 6.79 | 3.62 | 1.92 | 3.40 | 2.28 |
| Casa Forestal II | 3.47 | 0.00 | 1.73 | 7.42 | 7.84 | 5.79 | 2.16 | 5.21 | 3.94 |
| Casa Forestal V | 2.36 | 1.73 | 0.00 | 6.33 | 7.03 | 4.52 | 1.46 | 3.77 | 2.45 |
| Ceja de Piezarrodilla | 6.19 | 7.42 | 6.33 | 0.00 | 2.76 | 4.64 | 6.00 | 3.85 | 4.87 |
| Hoya de Navarejos II | 6.79 | 7.84 | 7.03 | 2.76 | 0.00 | 6.29 | 6.60 | 5.21 | 6.09 |
| Hoya de Navarejos III | 3.62 | 5.79 | 4.52 | 4.64 | 6.29 | 0.00 | 3.96 | 3.40 | 2.59 |
| Hoya de Navarejos V | 1.92 | 2.16 | 1.46 | 6.00 | 6.60 | 3.96 | 0.00 | 3.85 | 2.38 |
| La Cocinilla del Obispo | 3.40 | 5.21 | 3.77 | 3.85 | 5.21 | 3.40 | 3.85 | 0.00 | 2.05 |
| Prado Navazo | 2.28 | 3.94 | 2.45 | 4.87 | 6.09 | 2.59 | 2.38 | 2.05 | 0.00 |

Lower values indicate greater chemical similarity between locations.

**Table S9.** Statistical summary for the most discriminating individual elements in the white pigment samples.

| Element | F-statistic | df | p-value | $\eta^2$ |
|---|---|---|---|---|
| Ba | 20.892 | (5,43) | $1.557\times10^{-10}$ | 0.708 |
| Sr | 11.828 | (5,43) | $3.152\times10^{-7}$ | 0.579 |
| Si | 11.828 | (5,43) | $3.152\times10^{-7}$ | 0.579 |
| Mg | 11.828 | (5,43) | $3.152\times10^{-7}$ | 0.579 |
| Fe | 10.539 | (5,43) | $1.193\times10^{-6}$ | 0.551 |

**Table S10.** Mean Z-scores and standard deviations for the most discriminating elements in white pigment samples, organized by location.

| Location | Ba | Sr | Si | Mg | Fe |
|---|---|---|---|---|---|
| Ceja de Piezarrodilla | −1.106±0.334 | −1.333±0.340 | −1.333±0.340 | −1.333±0.340 | −0.337±0.359 |
| Hoya de Navarejos III | −0.703±0.309 | −0.902±0.384 | −0.902±0.384 | −0.902±0.384 | 0.119±0.306 |
| Prado Navazo | 1.493±0.703 | 1.497±1.308 | 1.497±1.308 | 1.497±1.308 | −0.727±0.688 |
| La Cocinilla del Obispo | 0.489±0.649 | −0.345±0.644 | −0.345±0.644 | −0.345±0.644 | −0.859±0.609 |
| Casa Forestal V | −0.363±0.493 | 0.603±0.430 | 0.603±0.430 | 0.603±0.430 | 0.668±0.343 |
| Casa Forestal II | −0.347±0.418 | −0.222±0.562 | −0.222±0.562 | −0.222±0.562 | 0.348±0.557 |

Note: Values are Z-scores of CLR-transformed data.

**Table S11.** Complete Cohen's d values for pairwise comparisons - white pigments.

| Element | Comparison | Cohen's d | p-value |
|---|---|---|---|
| Ba | Ceja de Piezarrodilla vs Prado Navazo | 3.55 | 4.404E−09 |
| Ba | Ceja de Piezarrodilla vs La Cocinilla del Obispo | 2.92 | NA |
| Ba | Ceja de Piezarrodilla vs Casa Forestal V | 3.45 | 3.872E−06 |
| Ba | Ceja de Piezarrodilla vs Casa Forestal II | 4.22 | 7.486E−09 |
| Ba | Hoya de Navarejos III vs Prado Navazo | 1.62 | 2.630E−03 |
| Ba | Hoya de Navarejos III vs La Cocinilla del Obispo | 1.40 | NA |
| Ba | Hoya de Navarejos III vs Casa Forestal V | 1.97 | 1.937E−02 |
| Ba | Hoya de Navarejos III vs Casa Forestal II | 2.70 | 9.650E−05 |
| Ba | Prado Navazo vs La Cocinilla del Obispo | 0.04 | 1.000E+00 |
| Ba | Prado Navazo vs Casa Forestal V | 0.87 | 1.000E+00 |
| Ba | Prado Navazo vs Casa Forestal II | 1.87 | 1.995E−01 |
| Ba | La Cocinilla del Obispo vs Casa Forestal V | 0.77 | 1.000E+00 |
| Ba | La Cocinilla del Obispo vs Casa Forestal II | 1.72 | 6.479E−01 |
| Ba | Casa Forestal V vs Casa Forestal II | 1.24 | 1.000E+00 |
| Sr | Ceja de Piezarrodilla vs Hoya de Navarejos III | 1.89 | NA |
| Sr | Ceja de Piezarrodilla vs Prado Navazo | 2.02 | 2.497E−05 |
| Sr | Ceja de Piezarrodilla vs La Cocinilla del Obispo | 0.83 | NA |
| Sr | Ceja de Piezarrodilla vs Casa Forestal V | 2.05 | 2.426E−04 |
| Sr | Ceja de Piezarrodilla vs Casa Forestal II | 2.55 | 1.781E−06 |
| Sr | Hoya de Navarejos III vs Prado Navazo | 0.21 | 1.000E+00 |
| Sr | Hoya de Navarejos III vs La Cocinilla del Obispo | 1.60 | NA |
| Sr | Hoya de Navarejos III vs Casa Forestal V | 0.91 | 1.000E+00 |
| Sr | Hoya de Navarejos III vs Casa Forestal II | 1.68 | 3.758E−01 |
| Sr | Prado Navazo vs La Cocinilla del Obispo | 1.53 | 4.577E−01 |
| Sr | Prado Navazo vs Casa Forestal V | 1.24 | 1.000E+00 |
| Sr | Prado Navazo vs Casa Forestal II | 2.08 | 1.285E−01 |
| Sr | La Cocinilla del Obispo vs Casa Forestal V | 3.62 | 1.075E−01 |
| Sr | La Cocinilla del Obispo vs Casa Forestal II | 4.91 | 4.200E−03 |
| Sr | Casa Forestal V vs Casa Forestal II | 1.21 | 1.000E+00 |
| Si | Ceja de Piezarrodilla vs Hoya de Navarejos III | 1.89 | NA |
| Si | Ceja de Piezarrodilla vs Prado Navazo | 2.02 | 2.497E−05 |
| Si | Ceja de Piezarrodilla vs La Cocinilla del Obispo | 0.83 | NA |
| Si | Ceja de Piezarrodilla vs Casa Forestal V | 2.05 | 2.426E−04 |
| Si | Ceja de Piezarrodilla vs Casa Forestal II | 2.55 | 1.781E−06 |
| Si | Hoya de Navarejos III vs Prado Navazo | 0.21 | 1.000E+00 |
| Si | Hoya de Navarejos III vs La Cocinilla del Obispo | 1.60 | NA |
| Si | Hoya de Navarejos III vs Casa Forestal V | 0.91 | 1.000E+00 |
| Si | Hoya de Navarejos III vs Casa Forestal II | 1.68 | 3.758E−01 |
| Si | Prado Navazo vs La Cocinilla del Obispo | 1.53 | 4.577E−01 |
| Si | Prado Navazo vs Casa Forestal V | 1.24 | 1.000E+00 |
| Si | Prado Navazo vs Casa Forestal II | 2.08 | 1.285E−01 |
| Si | La Cocinilla del Obispo vs Casa Forestal V | 3.62 | 1.075E−01 |
| Si | La Cocinilla del Obispo vs Casa Forestal II | 4.91 | 4.200E−03 |
| Si | Casa Forestal V vs Casa Forestal II | 1.21 | 1.000E+00 |
| Mg | Ceja de Piezarrodilla vs Hoya de Navarejos III | 1.89 | NA |
| Mg | Ceja de Piezarrodilla vs Prado Navazo | 2.02 | 2.497E−05 |
| Mg | Ceja de Piezarrodilla vs La Cocinilla del Obispo | 0.83 | NA |
| Mg | Ceja de Piezarrodilla vs Casa Forestal V | 2.05 | 2.426E−04 |
| Mg | Ceja de Piezarrodilla vs Casa Forestal II | 2.55 | 1.781E−06 |
| Mg | Hoya de Navarejos III vs Prado Navazo | 0.21 | 1.000E+00 |
| Mg | Hoya de Navarejos III vs La Cocinilla del Obispo | 1.60 | NA |
| Mg | Hoya de Navarejos III vs Casa Forestal V | 0.91 | 1.000E+00 |
| Mg | Hoya de Navarejos III vs Casa Forestal II | 1.68 | 3.758E−01 |
| Mg | Prado Navazo vs La Cocinilla del Obispo | 1.53 | 4.577E−01 |
| Mg | Prado Navazo vs Casa Forestal V | 1.24 | 1.000E+00 |
| Mg | Prado Navazo vs Casa Forestal II | 2.08 | 1.285E−01 |
| Mg | La Cocinilla del Obispo vs Casa Forestal V | 3.62 | 1.075E−01 |
| Mg | La Cocinilla del Obispo vs Casa Forestal II | 4.91 | 4.200E−03 |
| Mg | Casa Forestal V vs Casa Forestal II | 1.21 | 1.000E+00 |

**Table S11 (cont.).** Complete Cohen's d values for pairwise comparisons - white pigments.

| Element | Comparison | Cohen's d | p-value |
|---|---|---|---|
| Fe | Ceja de Piezarrodilla vs Hoya de Navarejos III | 0.21 | NA |
| Fe | Ceja de Piezarrodilla vs Prado Navazo | 1.80 | 6.722E−04 |
| Fe | Ceja de Piezarrodilla vs La Cocinilla del Obispo | 2.38 | NA |
| Fe | Ceja de Piezarrodilla vs Casa Forestal V | 1.36 | 4.522E−01 |
| Fe | Ceja de Piezarrodilla vs Casa Forestal II | 0.64 | 1.000E+00 |
| Fe | Hoya de Navarejos III vs Prado Navazo | 2.09 | 1.696E−05 |
| Fe | Hoya de Navarejos III vs La Cocinilla del Obispo | 2.80 | NA |
| Fe | Hoya de Navarejos III vs Casa Forestal V | 1.72 | 1.499E−01 |
| Fe | Hoya de Navarejos III vs Casa Forestal II | 0.93 | 1.000E+00 |
| Fe | Prado Navazo vs La Cocinilla del Obispo | 0.61 | 1.000E+00 |
| Fe | Prado Navazo vs Casa Forestal V | 0.43 | 1.000E+00 |
| Fe | Prado Navazo vs Casa Forestal II | 1.29 | 4.709E−01 |
| Fe | La Cocinilla del Obispo vs Casa Forestal V | 1.66 | 1.000E+00 |
| Fe | La Cocinilla del Obispo vs Casa Forestal II | 2.87 | 1.518E−01 |
| Fe | Casa Forestal V vs Casa Forestal II | 1.34 | 1.000E+00 |

### *Black and white-over-black pigments*

**Table S12.** Principal component analysis results for black and white-over-black pigment samples (n = 31).

| Component | Eigenvalue | % Variance | Cumulative % |
|---|---|---|---|
| 1 | 8.841 | 58.941 | 58.941 |
| 2 | 1.838 | 12.254 | 71.195 |
| 3 | 1.562 | 10.411 | 81.606 |
| 4 | 1.356 | 9.037 | 90.643 |

**Table S13**. Factor loadings from the principal component analysis of black, black-over-white, and white-over-black pigment samples.

| Element | Comp.1 | Comp.2 | Comp.3 |
|---|---|---|---|
| ZBa_CLR | −0.285 | 0.076 | −0.020 |
| ZBal_CLR | 0.276 | 0.285 | −0.259 |
| ZZr_CLR | 0.270 | −0.410 | 0.034 |
| ZSr_CLR | −0.287 | −0.074 | −0.091 |
| ZFe_CLR | 0.233 | 0.161 | 0.283 |
| ZMn_CLR | −0.282 | 0.155 | 0.028 |
| ZTi_CLR | 0.160 | −0.007 | 0.487 |
| ZCa_CLR | 0.183 | −0.068 | −0.555 |
| ZK_CLR | 0.177 | 0.419 | 0.381 |
| ZAl_CLR | 0.276 | 0.285 | −0.259 |
| ZP_CLR | 0.270 | −0.410 | 0.034 |
| ZSi_CLR | −0.287 | −0.074 | −0.091 |
| ZCl_CLR | 0.276 | 0.285 | −0.259 |
| ZS_CLR | 0.270 | −0.410 | 0.034 |
| ZMg_CLR | −0.287 | −0.074 | −0.091 |

**Table S14.** Sequential tests of discriminant functions for black, black-over-white, and white-over-black pigment samples.

| Functions tested | Wilks' Λ | $\chi^2$ | df | p-value |
|---|---|---|---|---|
| 1 through 5 | 0.000 | 268.16 | 75 | < 0.001 |
| 2 through 5 | 0.000 | 157.30 | 56 | < 0.001 |
| 3 through 5 | 0.007 | 96.68 | 39 | < 0.001 |
| 4 through 5 | 0.068 | 52.38 | 24 | < 0.001 |

**Table S15.** Structure matrix - correlations between elements and discriminant functions for black, black-over-white, and white-over-black pigment samples.

| Element | LD1 | LD2 | LD3 | LD4 | LD5 | Highest function |
|---|---|---|---|---|---|---|
| ZBa_CLR | −0.970 | 0.137 | 0.077 | 0.102 | 0.006 | 1 |
| ZBal_CLR | 0.672 | −0.173 | 0.027 | 0.200 | −0.411 | 1 |
| ZZr_CLR | 0.641 | −0.574 | −0.192 | 0.316 | 0.031 | 1 |
| ZSr_CLR | −0.799 | −0.047 | −0.191 | −0.277 | 0.393 | 1 |
| ZFe_CLR | 0.656 | −0.093 | 0.228 | −0.041 | −0.169 | 1 |
| ZMn_CLR | −0.618 | 0.565 | −0.140 | −0.401 | −0.06 | 1 |
| ZTi_CLR | 0.401 | −0.138 | 0.791 | 0.160 | 0.205 | 3 |
| ZCa_CLR | 0.515 | −0.260 | −0.147 | 0.292 | −0.112 | 1 |
| ZK_CLR | 0.533 | 0.458 | 0.185 | 0.195 | −0.127 | 1 |
| ZAl_CLR | 0.672 | −0.173 | 0.027 | 0.200 | −0.411 | 1 |
| ZP_CLR | 0.641 | −0.574 | −0.192 | 0.316 | 0.031 | 1 |
| ZSi_CLR | −0.799 | −0.047 | −0.191 | −0.277 | 0.393 | 1 |
| ZCl_CLR | 0.672 | −0.173 | 0.027 | 0.200 | −0.411 | 1 |
| ZS_CLR | 0.641 | −0.574 | −0.192 | 0.316 | 0.031 | 1 |
| ZMg_CLR | −0.799 | −0.047 | −0.191 | −0.277 | 0.393 | 1 |

**Table S16**. Pairwise Euclidean distance matrix between black, black-over-white, and white-over-black pigment sampling locations based on mean elemental compositions (n = 31 samples, 6 locations).

| | Cabras blancas | Ceja de Piezarrodilla | Hoya de Navarejos IV | Hoya de Navarejos III | La Cocinilla del Obispo | Prado Navazo |
|---|---|---|---|---|---|---|
| Cabras Blancas | 0.00 | 6.47 | 4.88 | 2.29 | 4.75 | 1.61 |
| Ceja de Piezarrodilla | 6.47 | 0.00 | 8.31 | 5.35 | 4.81 | 6.37 |
| Hoya de Navarejos IV | 4.88 | 8.31 | 0.00 | 4.03 | 7.20 | 4.45 |
| Hoya de Navarejos III | 2.29 | 5.35 | 4.03 | 0.00 | 4.50 | 2.18 |
| La Cocinilla del Obispo | 4.75 | 4.81 | 7.20 | 4.50 | 0.00 | 5.51 |
| Prado Navazo | 1.61 | 6.37 | 4.45 | 2.18 | 5.51 | 0.00 |

**Table S17.** Statistical summary for the most discriminating elements in the black, black-over-white, and white-over-black pigment samples.

| Element | F-statistic | df | p-value | $\eta^2$ |
|---|---|---|---|---|
| Ba | 105.135 | (3,24) | $6.088\times10^{-14}$ | 0.929 |
| Zr | 22.611 | (3,24) | $3.563\times10^{-7}$ | 0.739 |
| P | 22.611 | (3,24) | $3.563\times10^{-7}$ | 0.739 |
| S | 22.611 | (3,24) | $3.563\times10^{-7}$ | 0.739 |
| Mn | 21.413 | (3,24) | $5.716\times10^{-7}$ | 0.728 |

**Table S18.** Mean Z-scores and standard deviations for the five most discriminating individual elements in the black, black-over-white, and white-over-black pigment samples, organized by location.

| Location | Ba | Zr | P | S | Mn |
|---|---|---|---|---|---|
| Cabras Blancas | −0.538±0.118 | 0.651±0.249 | 0.651±0.249 | 0.651±0.249 | −0.640±0.037 |
| Ceja de Piezarrodilla | −0.542±0.230 | 1.059±0.864 | 1.059±0.864 | 1.059±0.864 | −0.511±0.613 |
| Hoya de Navarejos III | 1.273±0.213 | −1.456±0.644 | −1.456±0.644 | −1.456±0.644 | 1.692±0.343 |
| Prado Navazo | 0.342±0.407 | 0.044±0.573 | 0.044±0.573 | 0.044±0.573 | 0.084±1.433 |

Note: Values are Z-scores of CLR-transformed data.

**Table S19.** Complete Cohen's d values for pairwise comparisons – black, black-over-white, and white-over-black pigments.

| Element | Comparison | Cohen's d | p-value |
|---|---|---|---|
| Ba | Ceja de Piezarrodilla vs Hoya de Navarejos III | 3.39 | NA |
| Ba | Ceja de Piezarrodilla vs Prado Navazo | 9.08 | 3.459E-10 |
| Ba | Ceja de Piezarrodilla vs Cabras Blancas | 8.16 | 5.303E-14 |
| Ba | Hoya de Navarejos III vs Prado Navazo | 2.71 | 5.882E-04 |
| Ba | Hoya de Navarejos III vs Cabras Blancas | 3.14 | 1.510E-05 |
| Ba | Prado Navazo vs Cabras Blancas | 0.02 | 1.000E+00 |
| Zr | Ceja de Piezarrodilla vs Hoya de Navarejos III | 2.39 | NA |
| Zr | Ceja de Piezarrodilla vs Prado Navazo | 3.56 | 9.636E-04 |
| Zr | Ceja de Piezarrodilla vs Cabras Blancas | 3.28 | 1.743E-07 |
| Zr | Hoya de Navarejos III vs Prado Navazo | 1.29 | 1.000E+00 |
| Zr | Hoya de Navarejos III vs Cabras Blancas | 1.26 | 1.381E-01 |
| Zr | Prado Navazo vs Cabras Blancas | 0.51 | 1.000E+00 |
| P | Ceja de Piezarrodilla vs Hoya de Navarejos III | 2.39 | NA |
| P | Ceja de Piezarrodilla vs Prado Navazo | 3.56 | 9.636E-04 |
| P | Ceja de Piezarrodilla vs Cabras Blancas | 3.28 | 1.743E-07 |
| P | Hoya de Navarejos III vs Prado Navazo | 1.29 | 1.000E+00 |
| P | Hoya de Navarejos III vs Cabras Blancas | 1.26 | 1.381E-01 |
| P | Prado Navazo vs Cabras Blancas | 0.51 | 1.000E+00 |
| S | Ceja de Piezarrodilla vs Hoya de Navarejos III | 2.39 | NA |
| S | Ceja de Piezarrodilla vs Prado Navazo | 3.56 | 9.636E-04 |
| S | Ceja de Piezarrodilla vs Cabras Blancas | 3.28 | 1.743E-07 |
| S | Hoya de Navarejos III vs Prado Navazo | 1.29 | 1.000E+00 |
| S | Hoya de Navarejos III vs Cabras Blancas | 1.26 | 1.381E-01 |
| S | Prado Navazo vs Cabras Blancas | 0.51 | 1.000E+00 |
| Mn | Ceja de Piezarrodilla vs Hoya de Navarejos III | 2.07 | NA |
| Mn | Ceja de Piezarrodilla vs Prado Navazo | 7.5 | 1.364E-04 |
| Mn | Ceja de Piezarrodilla vs Cabras Blancas | 4.37 | 6.468E-07 |
| Mn | Hoya de Navarejos III vs Prado Navazo | 0.65 | 1.000E+00 |
| Mn | Hoya de Navarejos III vs Cabras Blancas | 0.68 | 8.725E-01 |
| Mn | Prado Navazo vs Cabras Blancas | 0.23 | 1.000E+00 |

### *Red pigments*

**Table S20.** Principal component analysis results for red pigment samples (n = 17).

| Component | Eigenvalue | % Variance | Cumulative % |
|---|---|---|---|
| 1 | 7.300 | 48.666 | 48.666 |
| 2 | 4.284 | 28.562 | 77.229 |
| 3 | 1.418 | 9.453 | 86.681 |

**Table S21**. Factor loadings from the principal component analysis of red pigment samples.

| Element | Comp.1 | Comp.2 | Comp.3 |
|---|---|---|---|
| ZBa_CLR | −0.242 | 0.149 | 0.108 |
| ZBal_CLR | 0.354 | −0.072 | 0.009 |
| ZZr_CLR | −0.219 | −0.333 | −0.338 |
| ZSr_CLR | −0.185 | 0.406 | −0.094 |
| ZFe_CLR | 0.22 | 0.224 | −0.076 |
| ZMn_CLR | −0.217 | −0.192 | 0.484 |
| ZTi_CLR | 0.237 | 0.139 | −0.303 |
| ZCa_CLR | 0.335 | −0.108 | 0.167 |
| ZK_CLR | 0.235 | 0.131 | −0.509 |
| ZAl_CLR | 0.354 | −0.072 | 0.009 |
| ZP_CLR | −0.219 | −0.333 | −0.338 |
| ZSi_CLR | −0.185 | 0.406 | −0.094 |
| ZCl_CLR | 0.354 | −0.072 | 0.009 |
| ZS_CLR | −0.219 | −0.333 | −0.338 |
| ZMg_CLR | −0.185 | 0.406 | −0.094 |

**Table S22.** Sequential tests of discriminant functions for red pigment samples.

| Functions tested | Wilks' Λ | $\chi^2$ | df | p-value |
|---|---|---|---|---|
| 1 through 4 | 0.000 | 84.58 | 60 | 0.020 |
| 2 through 4 | 0.000 | 50.04 | 42 | 0.185 |
| 3 through 4 | 0.009 | 28.37 | 26 | 0.340 |
| 4 through 4 | 0.118 | 12.83 | 12 | 0.381 |

**Table S23.** Structure matrix - correlations between elements and discriminant functions for red pigment samples.

| Element | LD1 | LD2 | LD3 | LD4 | Highest function |
|---|---|---|---|---|---|
| ZBa_CLR | −0.802 | 0.386 | 0.229 | 0.012 | 1 |
| ZBal_CLR | 0.643 | −0.548 | 0.043 | 0.351 | 1 |
| ZZr_CLR | −0.559 | −0.385 | 0.146 | −0.240 | 1 |
| ZSr_CLR | −0.310 | 0.846 | 0.145 | 0.297 | 2 |
| ZFe_CLR | 0.823 | 0.313 | 0.416 | 0.053 | 1 |
| ZMn_CLR | −0.354 | 0.016 | −0.469 | −0.784 | 4 |
| ZTi_CLR | 0.566 | −0.010 | −0.044 | 0.448 | 1 |
| ZCa_CLR | 0.602 | −0.540 | −0.236 | 0.281 | 1 |
| ZK_CLR | 0.496 | −0.085 | 0.144 | 0.691 | 4 |
| ZAl_CLR | 0.643 | −0.548 | 0.043 | 0.351 | 1 |
| ZP_CLR | −0.559 | −0.385 | 0.146 | −0.240 | 1 |
| ZSi_CLR | −0.310 | 0.846 | 0.145 | 0.297 | 2 |
| ZCl_CLR | 0.643 | −0.548 | 0.043 | 0.351 | 1 |
| ZS_CLR | −0.559 | −0.385 | 0.146 | −0.240 | 1 |
| ZMg_CLR | −0.310 | 0.846 | 0.145 | 0.297 | 2 |

**Table S24**. Pairwise Euclidean distance matrix between red pigment sampling locations based on mean elemental compositions (n = 17 samples, 5 locations).

| | Casa Forestal II | Hoya de Navarejos III | Hoya de Navarejos V | La Cocinilla del Obispo | Tío Campano |
|---|---|---|---|---|---|
| Casa Forestal II | 0.00 | 6.97 | 3.69 | 4.22 | 3.08 |
| Hoya de Navarejos III | 6.97 | 0.00 | 5.11 | 5.52 | 8.07 |
| Hoya de Navarejos V | 3.69 | 5.11 | 0.00 | 1.62 | 3.94 |
| La Cocinilla del Obispo | 4.22 | 5.52 | 1.62 | 0.00 | 3.89 |
| Tío Campano | 3.08 | 8.07 | 3.94 | 3.89 | 0.00 |

**Table S25.** Statistical summary for the most discriminating elements in the red pigment samples.

| Element | F-statistic | df | p-value | $\eta^2$ |
|---|---|---|---|---|
| Fe | 25.147 | (3,12) | $1.840\times10^{-5}$ | 0.863 |
| Sr | 19.937 | (3,12) | $5.910\times10^{-5}$ | 0.833 |
| Si | 19.937 | (3,12) | $5.910\times10^{-5}$ | 0.833 |
| Mg | 19.937 | (3,12) | $5.910\times10^{-5}$ | 0.833 |
| Ba | 15.950 | (3,12) | $1.734\times10^{-4}$ | 0.799 |

**Table S26.** Mean Z-scores and standard deviations for the most discriminating elements in red pigment samples, organized by location.

| Location | Fe | Sr | Si | Mg | Ba |
|---|---|---|---|---|---|
| Tío Campano | 0.539±0.446 | −1.246±0.419 | −1.246±0.419 | −1.246±0.419 | −1.226±0.267 |
| La Cocinilla del Obispo | 0.873±0.219 | −0.066±0.306 | −0.066±0.306 | −0.066±0.306 | 0.209±0.186 |
| Hoya de Navarejos V | 0.803±0.546 | 0.326±0.099 | 0.326±0.099 | 0.326±0.099 | −0.214±0.687 |
| Casa Forestal II | 3.093±0.441 | −0.676±0.359 | −0.676±0.359 | −0.676±0.359 | −1.487±0.183 |

Note: Values are Z−scores of CLR−transformed data.

**Table S27.** Complete Cohen's d values for pairwise comparisons − red pigments.

| Element | Comparison | Cohen's d | p−value |
|---|---|---|---|
| Fe | Tío Campano vs La Cocinilla del Obispo | 4.52 | 9.029E−05 |
| Fe | Tío Campano vs Hoya de Navarejos V | 6.81 | 1.218E−04 |
| Fe | Tío Campano vs Casa Forestal II | 5.75 | 1.925E−05 |
| Fe | La Cocinilla del Obispo vs Hoya de Navarejos V | 0.17 | 1.000E+00 |
| Fe | La Cocinilla del Obispo vs Casa Forestal II | 0.54 | 1.000E+00 |
| Fe | Hoya de Navarejos V vs Casa Forestal II | 0.91 | 1.000E+00 |
| Sr | Tío Campano vs La Cocinilla del Obispo | 4.18 | 9.890E−03 |
| Sr | Tío Campano vs Hoya de Navarejos V | 1.86 | 1.806E−01 |
| Sr | Tío Campano vs Casa Forestal II | 1.43 | 2.013E−01 |
| Sr | La Cocinilla del Obispo vs Hoya de Navarejos V | 1.72 | 6.837E−01 |
| Sr | La Cocinilla del Obispo vs Casa Forestal II | 4.87 | 6.443E−05 |
| Sr | Hoya de Navarejos V vs Casa Forestal II | 3.15 | 9.426E−04 |
| Si | Tío Campano vs La Cocinilla del Obispo | 4.18 | 9.890E−03 |
| Si | Tío Campano vs Hoya de Navarejos V | 1.86 | 1.806E−01 |
| Si | Tío Campano vs Casa Forestal II | 1.43 | 2.013E−01 |
| Si | La Cocinilla del Obispo vs Hoya de Navarejos V | 1.72 | 6.837E−01 |
| Si | La Cocinilla del Obispo vs Casa Forestal II | 4.87 | 6.443E−05 |
| Si | Hoya de Navarejos V vs Casa Forestal II | 3.15 | 9.426E−04 |
| Mg | Tío Campano vs La Cocinilla del Obispo | 4.18 | 9.890E−03 |
| Mg | Tío Campano vs Hoya de Navarejos V | 1.86 | 1.806E−01 |
| Mg | Tío Campano vs Casa Forestal II | 1.43 | 2.013E−01 |
| Mg | La Cocinilla del Obispo vs Hoya de Navarejos V | 1.72 | 6.837E−01 |
| Mg | La Cocinilla del Obispo vs Casa Forestal II | 4.87 | 6.443E−05 |
| Mg | Hoya de Navarejos V vs Casa Forestal II | 3.15 | 9.426E−04 |
| Ba | Tío Campano vs La Cocinilla del Obispo | 2.34 | 7.150E−03 |
| Ba | Tío Campano vs Hoya de Navarejos V | 9.19 | 6.732E−04 |
| Ba | Tío Campano vs Casa Forestal II | 1.08 | 1.000E+00 |
| Ba | La Cocinilla del Obispo vs Hoya de Navarejos V | 0.84 | 9.332E−01 |
| Ba | La Cocinilla del Obispo vs Casa Forestal II | 2.05 | 1.474E−02 |
| Ba | Hoya de Navarejos V vs Casa Forestal II | 6.08 | 9.394E−04 |

**References** (reference numbers do not match those that appear in the main document)


1. Obermaier, H. Nuevas pinturas rupestres descubiertas en los alrededores de Tormón (Teruel). *Investigación y Progreso* **1927**, *I*, 1−2.
2. Obermaier, H.; Breuil, H. Las pinturas rupestres de los alrededores de Tormón (Teruel). *Boletín de la Real Academia de la Historia* **1927**, *90*, 511−531.
3. Beltrán Martínez, A. *Arte Rupestre Levantino*; Universidad de Zaragoza: Zaragoza, Spain, 1968; Vol. IV.
4. Beltrán Martínez, A. *Arte prehistórico en Aragón*; Ibercaja: Zaragoza, Spain, 1993; pp. 228.
5. Piñón Varela, F. Superposiciones y repintados en la serranía de Albarracín: elementos para el establecimiento de una cronología relativa. In *Altamira Symposium*, Ministerio de Cultura, Dirección General de Archivos, Bibliotecas y Museos: Madrid, Spain, 1981; pp. 411−426.
6. Piñón Varela, F. *Las pinturas rupestres de Albarracín (Teruel)*; Dirección General de Bellas Artes, Archivos y Bibliotecas: Santander, Spain, 1982; Vol. 6.
7. Bea Martínez, M.; Angás Pajas, J.G.S., Luis Miguel; Gutiérrez, F.J.; Longares Aladrén, L.A.M., Salvador; Peña Monné, J.L. *Las pinturas rupestres de Bezas y Tormón (Teruel)*; Bea Martínez, M., Angás Pajas, J., Eds.; Parque Cultural de Albarracín: Teruel, Spain, 2015; pp. 182.
8. Bea Martínez, M. El abrigo de Hoya de Navarejos III (Tormón, Teruel). Nuevas perspectivas para el análisis del arte levantino interior. *Complutum* **2017**, *28*, 37−50, doi:10.5209/CMPL.58417.